Using adaptive filtering to track long-transient gravitational waves with varying frequency and amplitude

Rebecca White
Dornsife College of Letters, Arts and Sciences, University of Southern California, Los Angeles, California 90089, USA

Mentor: Ling Sun
LIGO Laboratory, California Institute of Technology, Pasadena, California 91125, USA and
OzGrav-ANU, Centre for Gravitational Astrophysics, College of Science,
The Australian National University, ACT 2601, Australia
(Dated: November 1, 2020)

Advanced Laser Interferometer Gravitational-Wave Observatory (LIGO) and Virgo have observed transient gravitational wave (GW) signals from compact binary coalescences. Yet undetected GWs from other types of sources, including quasimonochromatic continuous waves (CW) from individual spinning neutron stars and long-transient signals from newly born neutron stars, are of interest. We explore the capability of an adaptive filter, named "iWave", to track and detect weak CW or long-transient GW signals and quantify the sensitivity. This new tracking method, operating on time-series data, provides an efficient alternative to existing frequency-domain matched filter search methods. We demonstrate that it can be used in follow-ups of binary neutron star postmerger remnants. Further, we discuss the application of iWave to tracking and removing narrow-band instrumental spectral lines from the interferometric data, which could obscure astrophysical signals at the frequencies where they occur.

I. INTRODUCTION

On September 14th, 2015, Advanced Laser Interferometer Gravitational-Wave Observatory (LIGO) detected its first gravitational wave (GW) event, GW150914 [1]. This event was detected in the first observing run (O1) of Advanced LIGO (from September 12th, 2015 to January 19th, 2016). After O1 concluded, the second observing run (O2) began on November 30th, 2016 and ended on August 25th, 2017 [2]. During the O2 run, the binary neutron star (BNS) merger event, GW170817, was detected [3]. In the third observing run (O3), an increased number of merger candidates were identified [**?**], including events of particular interest: GW190412 [4], GW190425 [5], GW190521 [6], and GW190814 [7]. Throughout the entire O1–O3 runs, all of the GW events are from compact binary coalescences (CBCs), most of which are binary black hole (BBH) mergers.

There are other types of GWs in addition to those from CBCs. Continuous waves (CWs) are produced by individual spinning neutron stars. There are also long-transient GW signals that can be produced by a post-merger remnant from a BNS merger. Burst GWs are not yet very well understood since they are difficult to model. Once detected, however, they will be able to reveal a significant amount of astrophysical information. Stochastic background GWs from the early evolution of the universe are another type of weak signals remaining to be detected [8].

The raw data from the LIGO detectors contain noise and glitches, so one of the most important aspects of LIGO data analysis is detector characterization and noise modeling. Without being able to monitor the detector or track the noise accurately, the significance of an event could be incorrectly estimated. A significant part of LIGO noise is instrumental lines, which can obscure astrophysical signals at the frequencies where they occur. They cannot be factored out easily and some are not very well understood. Some may even have wandering frequencies and/or varying amplitudes, which makes them even more difficult to track [9].

Adaptive filtering is a dynamic approach for characterizing the features in input data, including noise lines or signals with wandering frequencies and amplitudes. This method is very helpful when the input signal changes over a period of time. It could prove helpful in analyzing the detector interferometric data, tracking the varying instrumental lines over the run. A phase locked loop (PLL) is a control system that uses an oscillator to produce an output signal at a frequency and phase synchronized with the input signal. "iWave" is a hybrid method of a traditional PLL and an adaptive filter that is used for signal tracking. This allows us to combine the wandering frequency/amplitude aspects of adaptive filters with the oscillation frequencies of PLLs to help us better track signals over a period of time. Existing techniques, e.g., the hidden Markov model tracking, can also track wandering signals and has been used for tracking both instrumental lines as well as CW and long-transient GWs [10–12]. Such methods mainly work in the frequency domain while iWave could prove to be an alternative method for analyzing the data in the time domain.

In this paper, we present how iWave tracks long-transient GW signals. In Section II, we explain the iWave method in more detail and show testing examples. Section III describes the long-transient GW signal model and the capability of iWave to recover synthetic signals injected in Gaussian noise. In Section IV, we briefly discuss another application of iWave: tracking and removing

spectral noise lines in interferometric data. Finally, we conclude in Section V.

II. IWAVE

A. Algorithm

A traditional PLL is a loop containing a voltage-controlled oscillator (VCO), a loop filter (LF), and a phase detector (PD). The VCO is an oscillator set to a frequency ω which controls the signal. The VCO input is set by the output of the PD since the PD determines the phase difference between the oscillating input and the VCO output. The LF controls the bandwidth of the PLL. However, there are two relevant limitations when using PLLs — (1) the input signal amplitude, and (2) an oscillating component introduced by the PD. Traditional PLLs do not determine the input amplitude and the output of the PLL is not related to the amplitude of the input. This amplitude information is crucial for GW signal tracking and noise subtraction. The second flaw with using only a traditional PLL is that the PD introduces an oscillating component at 2ω. This needs to be filtered out before being fed into the VCO, because otherwise there will be sidebands in the output. Through filtering it out, a phase shift could occur and cause more issues with the output.

iWave is a PLL in which the reference oscillator is replaced by an adaptive filter, making it a hybrid of a traditional PLL and an adaptive filter. It utilizes a resonant orthogonal system generator to produce two oscillating outputs — d_{out} being in-phase with the input and q_{out} being 90 degrees out of phase (the quadrature phase). The bandwidth of iWave is set using a single response time parameter so the phases will automatically line up. iWave is a technique for dynamically characterizing oscillations whose amplitudes and frequencies may vary. Unlike traditional PLLs, it can calculate the amplitude of the input signal using its two outputs through the equation [13]

$$A_{\text{out}} = \sqrt{d_{\text{out}}^2 + q_{\text{out}}^2}. \tag{1}$$

iWave is meant to characterize the oscillating input x_n through the output y_n. The iteration equation for the output of iWave is given by [13]

$$y_n = e^{-w} e^{i\Delta} y_{n-1} + (1 - e^{-w}) x_n, \tag{2}$$

Where $1/w$ is the number of samples corresponding to one e-folding in the relative weight of previous samples, Δ is the frequency in radians per sample, y_{n-1} is the previous output, and x_n is the input.

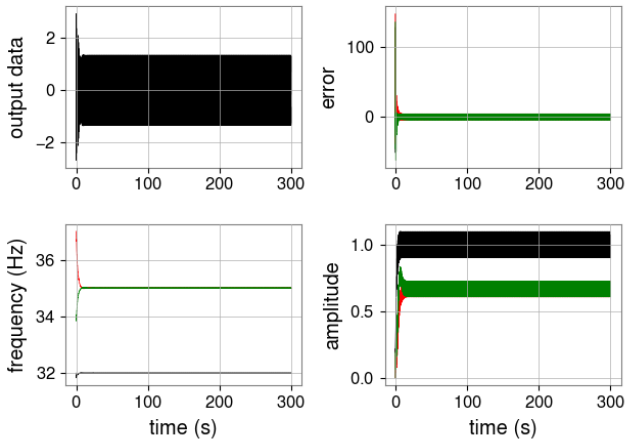

FIG. 1. iWave multi-line tracking test. The four plots each represent a different output of iWave. The top left plot is the output data in the time domain. The top right is the internal error calculated for the estimation. The bottom left and right are the frequency and amplitude estimations respectively. Each colored line is a different iteration of iWave trying to track one of the lines with different f_{guess} values. The red line starts at a frequency of 37 Hz, green line at 34 Hz, and black line at 32 Hz. As shown in the bottom left plot, iWave only locks onto the 32 Hz and 35 Hz signals since those are the closest lines to the f_{guess} values despite this meaning that the 35-Hz line is tracked twice. The τ value was set to 1 s.

B. Tracking example

The two input parameters of iWave that have an effect on its ability to track are the initial guess of the signal frequency, f_{guess}, and the characteristic timescale of the signal, τ. In order to better understand how iWave works in relation to these parameters, tests were done with different iWave f_{guess} and τ values in multiple circumstances.

In order to test iWave's responses to different f_{guess} values, a multi-line tracking test was conducted. This test was done with signals at 30 Hz, 32 Hz, and 35 Hz without additive noise. When the f_{guess} values matched the true signal frequencies, iWave locked on to all of the lines immediately. However, if the f_{guess} values were changed to the point where two f_{guess} values were closer to a single line than either of the other lines, iWave would track the same line twice. This duplication can be clearly seen in Figure 1 where the 35-Hz line is tracked twice since the f_{guess} values were set to 32 Hz, 34 Hz, and 37 Hz. This implies that, when tracking signals at close frequencies, setting f_{guess} close to the true values is important to avoid duplicated tracking.

Another test that was done with iWave involved tracking a synthetic GW signal within noise. The main purpose of this test was to clearly see the effect of τ on iWave's ability to track this signal with varying frequency. The synthetic signal starts at 1000 Hz, so we

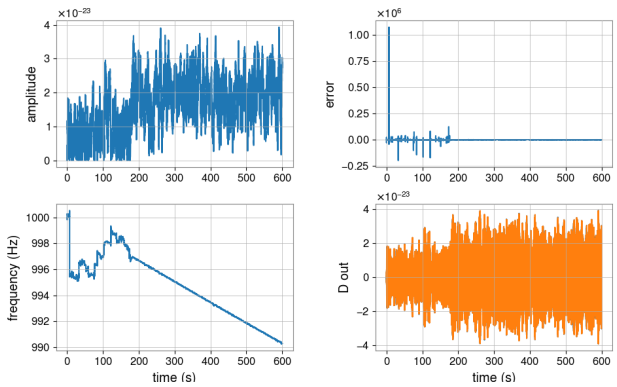

FIG. 2. iWave outputs for injected signal in Gaussian noise when $\tau = 1.5$ s and $f_{\rm guess} = 1000$ Hz. The top left plot is the amplitude estimate of the signal. The top right plot is the error of the estimation. The bottom left plot shows the frequency estimate. The bottom right plot is the iWave in-phase output. As shown in the error and frequency plots, iWave tracks the evolving signal in the simulated time-series and can lock on to the signal after ~ 180 s.

fix $f_{\rm guess}$ at 1000 Hz. A set of τ values, 0.1 s, 0.5 s, 1.0 s, 1.5 s, and 2.0 s, were tested. In this case, a τ value of 1.5 s yielded the smallest frequency-based root-mean-square (RMS) error once iWave locked onto the signal. Figure 2 shows the iWave output for this test with $\tau = 1.5$ s. These test results indicate that, when tracking a signal, different iWave τ values should be tested in order to obtain the optimal tracking results.

III. TRACKING LONG-TRANSIENT GW SIGNALS

A. Signal model

Our search using iWave does not rely on a particular signal model in order to be successful in tracking an evolving signal. However, we still need a set of modeled synthetic signals to test iWave's abilities. Hence, we simulate signals using a model that has been used in other studies searching for GW signals from BNS post-merger remnants [14, 15]. This model describes the expected GW signals from a rapidly spinning-down millisecond magnetar born after a BNS merger [16]. The time-dependent GW frequency is given by [15, 16]

$$f_{\rm gw}(t) = f_0(1 + \frac{t}{\tau_{\rm gw}})^{\frac{1}{1-n}}, \tag{3}$$

where $\tau_{\rm gw}$ is the spin-down timescale, f_0 is the initial GW frequency at $t = 0$ s, and n is the breaking index. A braking index of $n = 5$ is preferred in our study because it simulates the signal from a source whose energy loss is dominated by GW emission. The GW strain amplitude is [15, 16]

$$h_0(t) = \frac{4\pi^2 G}{c^4}\frac{I_{zz}\epsilon}{d} f_{\rm gw}^2(t), \tag{4}$$

where G is Newton's gravitational constant, c is the speed of light, I_{zz} is the principal moment of inertia, ϵ is the mass ellipticity of the remnant, and d is the distance to the source.

B. Tracking results

Using synthetic signals described in Section III A, we test iWave's sensitivity. In our experiments, we inject the signal into Gaussian noise. Similar tests in detector noise remain to be conducted. All of the simulations described in this section are based on a set of fixed parameters: $f_0 = 2000$ Hz, $\tau_{\rm gw} = 10000$ s, $n = 5$, $\epsilon = 0.01$, and $I_{zz} = 10^{45}$ g cm^2. We test iWave's sensitivity by varying parameter d and quantifying the maximum d at which the signal can be recovered. Figure 3–5 show the iWave output plotted on top of the simulated signal at various distances.

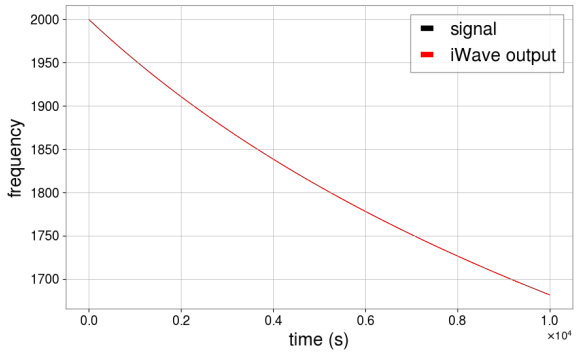

FIG. 3. Simulated signal and iWave output frequency ($d = 1$ Mpc). The black curve indicates the signal frequency as a function of time. The red curve is the estimated signal frequency from iWave. The iWave output matches the injection throughout the entire tracking period.

We tested d values from 1 Mpc to 10 Mpc. As shown in Figure 3, the estimated frequency perfectly matches the injection. This same level of matching is found until d is enlarged to 8 Mpc, where iWave only partially recovers the injected signal path. Figure 4 plots the estimated frequency over the injected signal path when $d = 8$ Mpc. Towards the end of the tracking period, there is some inconsistency between the output and the signal. For $d > 8$Mpc, iWave begins to completely lose the signal after a period of time. This is evident when d is set to 10 Mpc as shown in Figure 5. The reason why iWave starts to lose the signal near the ends is because the amplitude of the signal (h_0) decreases with time. Sometimes, because of this decrease in amplitude, the length

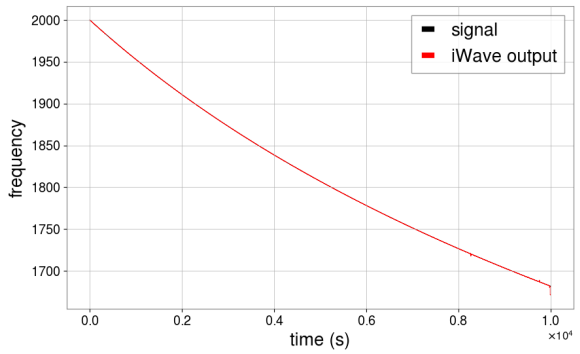

FIG. 4. Simulated signal and iWave output frequency (d = 8 Mpc). The black curve indicates the signal frequency as a function of time. The red curve is the estimated signal frequency from iWave. The iWave output matches the injection for most of the tracking period and only loses the signal slightly towards the end of the tracking period.

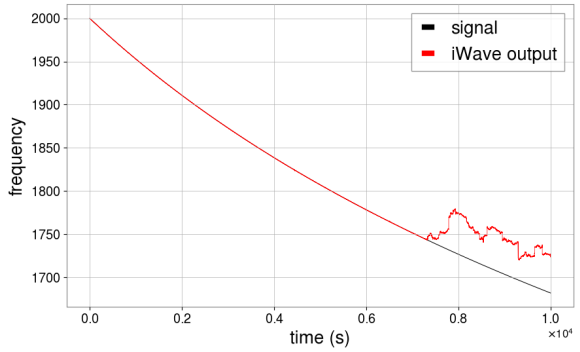

FIG. 5. Simulated signal and iWave output frequency (d = 10 Mpc). The black curve indicates the signal frequency as a function of time. The red curve is the estimated signal frequency from iWave. The iWave output matches the injection at the beginning and completely loses the signal at the end of the tracking period.

of the signal observing time ends up harming the accuracy since the amplitude will be too small to pick up within the noise. Because of this, we need to find an optimal tracking duration.

In order to quantify how accurate iWave is in its frequency tracking, Figure 6 plots the RMS error as a function of source distance with different signal timescales. A smaller $\tau_{\rm gw}$ value indicates that the signal evolves more rapidly. We tested $\tau_{\rm gw}$ values of 10^2 s, 10^3 s, 10^4 s, and 10^5 s. The other parameters are fixed: $f_0 = 2000$ Hz, $n = 5$, $\epsilon = 0.01$, and $I_{zz} = 10^{45}$ g cm^2. It is shown that iWave is better at tracking longer signals that do not evolve rapidly. The sensitivity limits seem to be consistent with other studies based on the same signal model. However, we are currently only testing iWave with one detector at a time, so we hope that iWave's sensitivity will improve with inputs from multiple detectors. We also wish to run these simulations in real detector noise instead of Gaussian noise. Also, a detection statistic is still missing from these simulations. While iWave seems to be comparable to other methods with this initial premature comparison, iWave is not sensitive enough to be able to track remnant from GW170817 since it was 40 Mpc away. However, using iWave is a good starting point in preparation for future BNS events.

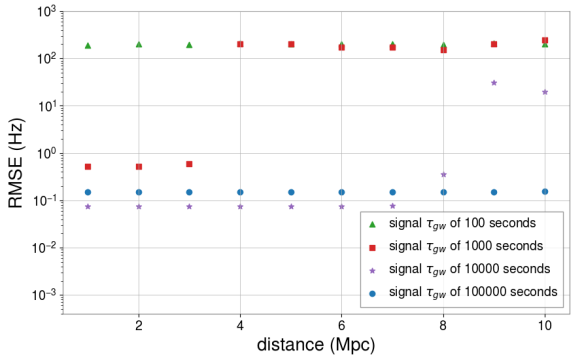

FIG. 6. RMS error in frequency as a function of source distance. The markers indicate the signal spin-down timescale $\tau_{\rm gw}$, as shown in the legend. The limits for iWave to accurately recover a signal is at $d \approx 3$ Mpc and $d \approx 8$ Mpc for $\tau_{\rm gw} = 10^3$ s and $\tau_{\rm gw} = 10^4$ s, respectively.

IV. DISCUSSION

Another possible application of iWave is tracking and removing spectral noise lines. In order to test this application, we had iWave track the 120-Hz power main line harmonic in the Livingston strain data starting at GPS time 1241136018 and ending 600 s after. We used a bandpass filter with a lower bound of 115 Hz and a higher bound of 125 Hz so that iWave can focus on the frequency band where the 120-Hz power main line is to avoid louder lines nearby. Figure 7 shows the filtered data compared to the cleaned data after subtracting iWave's output from the filtered data. As shown in the figure, the cleaned data no longer contain the peak at 120 Hz.

Figure 8 shows the iWave output in this tracking example. The 120-Hz power line can fluctuate slightly in frequency over the time period, so the wandering estimated frequency seems normal. However, for a while the amplitude estimates were inaccurate — being smaller than the raw/filtered data by an order of magnitude. This has recently been investigated and confirmed to be an impact from the τ value chosen. We have $\tau = 4.5$ in this test, which does not satisfy the requirement.

Only limited and preliminary tests have been conducted to test the capabilities of iWave in noise line subtraction. These preliminary studies seem promising. Further studies remain to be carried out.

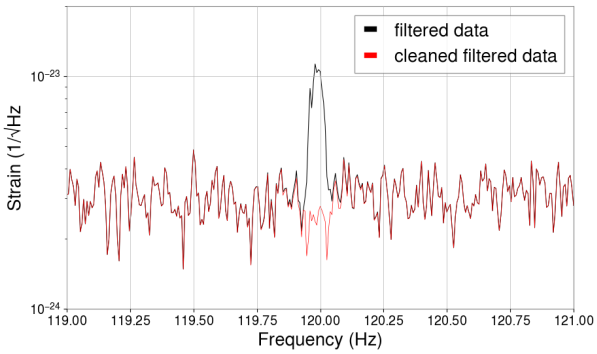

FIG. 7. Example of data cleaning with iWave. The black curve indicates the 120-Hz power main line harmonic after passing through a bandpass filter. The red curve is the cleaned data after subtracting the output of iWave.

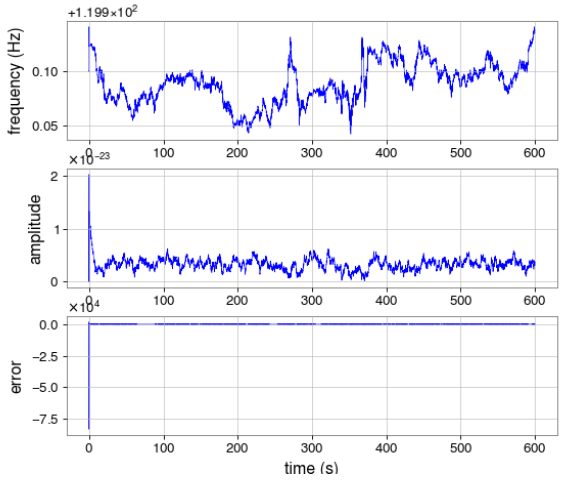

FIG. 8. iWave tracking of the 120-Hz power main line. The top panel is the frequency estimate; it is as expected that the line frequency wanders. The middle panel shows the amplitude estimate. The bottom panel is the error of the estimation.

V. CONCLUSION

In this article, we present a preliminary study to use an adaptive hybrid filter, iWave, as an alternative method to search for long-transient GW signals in time domain. We show preliminary test results, demonstrate how iWave tracks long-transient GW signals, quantify the sensitivity in Gaussian noise simulations, and discuss how to improve the implementation. We also discuss the possibility of using iWave to track and remove spectral noise lines. We hope to fully implement iWave as a time-domain GW signal tracking method and a noise subtraction tool in future GW data analyses after a more thorough study of this method.

VI. ACKNOWLEDGMENTS

The authors thank Edward Daw, Max Fays, Ian Hollows, and Timesh Minstry for their guidance with iWave. RW would like to thank Ling Sun for her guidance and mentorship throughout this project. RW would also like to thank Alan Weinstein, the Student-Faculty Program, and the fellow LIGO SURF students for making the LIGO SURF program possible. Finally, RW acknowledges support from the National Science Foundation Research Experience for Undergraduates.

[1] B P Abbott and others. Observation of gravitational waves from a binary black hole merger. *Phys. Rev. Lett.*, 116:061102, Feb 2016.

[2] B P Abbott and others. GWTC-1: A Gravitational-Wave Transient Catalog of Compact Binary Mergers Observed by LIGO and Virgo during the First and Second Observing Runs. *Phys. Rev. X*, 9:031040, Sep 2019.

[3] B P Abbott and others. GW170817: Observation of Gravitational Waves from a Binary Neutron Star Inspiral. *Phys. Rev. Lett.*, 119:161101, Oct 2017.

[4] B P Abbott and others. GW190412: Observation of a binary-black-hole coalescence with asymmetric masses. *Phys. Rev. D*, 102:043015, Aug 2020.

[5] B P Abbott and others. GW190425: Observation of a compact binary coalescence with total mass ~ 3.4 m $\odot$. *The Astrophysical Journal*, 892(1):L3, mar 2020.

[6] R. Abbott et al. GW190521: A Binary Black Hole Merger with a Total Mass of 150 $M_{\odot}$. *Phys. Rev. Lett.*, 125:101102, Sep 2020.

[7] B P Abbott and others. GW190814: Gravitational waves from the coalescence of a 23 solar mass black hole with a 2.6 solar mass compact object. *The Astrophysical Journal*, 896(2):L44, jun 2020.

[8] Sources and types of gravitational waves.

[9] B P Abbott et al. A guide to LIGO–virgo detector noise and extraction of transient gravitational-wave signals. *Classical and Quantum Gravity*, 37(5):055002, feb 2020.

[10] S. Suvorova, L. Sun, A. Melatos, W. Moran, and R. J. Evans. Hidden markov model tracking of continuous

gravitational waves from a neutron star with wandering spin. *Phys. Rev. D*, 93:123009, Jun 2016.

[11] Ling Sun and Andrew Melatos. Application of hidden markov model tracking to the search for long-duration transient gravitational waves from the remnant of the binary neutron star merger gw170817. *Phys. Rev. D*, 99:123003, Jun 2019.

[12] Joe Bayley, Chris Messenger, and Graham Woan. Generalized application of the viterbi algorithm to searches for continuous gravitational-wave signals. *Phys. Rev. D*, 100:023006, Jul 2019.

[13] E J Daw, T B Edo, I J Hollows, R Kennedy, and T Mistry. IWAVE – An adaptive filter approach to phase lock and the dynamic characterisation of pseudo-harmonic waves. 2020 in prep.

[14] B. P. Abbott et al. Search for gravitational waves from a long-lived remnant of the binary neutron star merger GW170817. *The Astrophysical Journal*, 875(2):160, apr 2019.

[15] Ling Sun and Andrew Melatos. Application of hidden Markov model tracking to the search for long-duration transient gravitational waves from the remnant of the binary neutron star merger GW170817. *Phys. Rev. D*, 99:123003, Jun 2019.

[16] Paul D. Lasky, Cristiano Leris, Antonia Rowlinson, and Kostas Glampedakis. The Braking Index of Millisecond Magnetars. *The Astrophysical Journal Letters*, jul 2017.